AD-A174 544 ACTIVE FEEDBACK INTERACTION WITH A SHEAR LAYER(U) 1/1
CALIFORNIA INST OF TECH PASADENA GRADUATE AERONAUTICAL
LABS P E DIMOTAKIS ET AL. 30 JUN 86 AFOSR-TR-86-1034
UNCLASSIFIED AFOSR-84-0120 F/G 20/4 NL

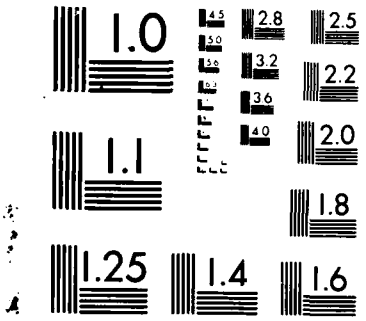

MICROCOPY RESOLUTION TEST CHART
NATIONAL BUREAU OF STANDARDS-1963-A

AFOSR-TR- 86-1034

(2)

GRADUATE AERONAUTICAL LABORATORIES
CALIFORNIA INSTITUTE OF TECHNOLOGY

ACTIVE FEEDBACK INTERACTION WITH A SHEAR LAYER

by

P. E. Dimotakis and M. M. Koochesfahani

AFOSR Grant No. AFOSR-84-0120

Annual Progress Report

for the period June 1985 - June 1986

Firestone Flight Sciences Laboratory

Guggenheim Aeronautical Laboratory

Karman Laboratory of Fluid Mechanics and Jet Propulsion

Pasadena

Unclassified

SECURITY CLASSIFICATION OF THIS PAGE

REPORT DOCUMENTATION PAGE

1a. REPORT SECURITY CLASSIFICATION Unclassified	1b. RESTRICTIVE MARKINGS None
2a. SECURITY CLASSIFICATION AUTHORITY	3. DISTRIBUTION/AVAILABILITY OF REPORT Distribution unlimited; approved for public release
2b. DECLASSIFICATION/DOWNGRADING SCHEDULE	
4. PERFORMING ORGANIZATION REPORT NUMBER(S)	5. MONITORING ORGANIZATION REPORT NUMBER(S) AFOSR-TR- 86-1034
6a. NAME OF PERFORMING ORGANIZATION California Institute of Technology 6b. OFFICE SYMBOL (If applicable)	7a. NAME OF MONITORING ORGANIZATION Air Force Office of Scientific Research
6c. ADDRESS (City, State and ZIP Code) Pasadena, CA 91125	7b. ADDRESS (City, State and ZIP Code) Bolling AFB, DC 20332
8a. NAME OF FUNDING/SPONSORING ORGANIZATION Air Force Office of Scientific Research 8b. OFFICE SYMBOL (If applicable) AFOSR/NA	9. PROCUREMENT INSTRUMENT IDENTIFICATION NUMBER AFOSR-84-0120
8c. ADDRESS (City, State and ZIP Code) Bolling AFB, DC 20332	10. SOURCE OF FUNDING NOS. PROGRAM ELEMENT NO. 61102F; PROJECT NO. 2307; TASK NO. A2; WORK UNIT NO.
11. TITLE (Include Security Classification) (Unclassified) Active Feedback Interaction with a Shear Layer	
12. PERSONAL AUTHOR(S) P. E. Dimotakis and M. M. Koochesfahani	
13a. TYPE OF REPORT Annual Progress Rpt. 13b. TIME COVERED FROM June 85 TO June 86	14. DATE OF REPORT (Yr., Mo., Day) 30 June 1986 15. PAGE COUNT 24
16. SUPPLEMENTARY NOTATION	
17. COSATI CODES FIELD / GROUP / SUB. GR.	18. SUBJECT TERMS (Continue on reverse if necessary and identify by block number) Shear flow, unsteady airfoil, active control, turbulence

19. ABSTRACT (Continue on reverse if necessary and identify by block number)

Work is continuing on the characterization of the effects of a pitching airfoil on the shear layer structure and growth under open loop forcing. We have shown that locally introduced disturbances can induce significant changes in the growth of the shear layer mixing zone. A separate investigation into the structure of the wake of an oscillating airfoil in a steady, uniform free stream revealed the existence of an axial flow along the cores of the wake vortices. The magnitude of the axial flow appears to depend on both the frequency and amplitude of oscillation.

20. DISTRIBUTION/AVAILABILITY OF ABSTRACT UNCLASSIFIED/UNLIMITED ☒ SAME AS RPT. ☐ DTIC USERS ☐	21. ABSTRACT SECURITY CLASSIFICATION Unclassified
22a. NAME OF RESPONSIBLE INDIVIDUAL Dr. Jim McMichael	22b. TELEPHONE NUMBER (Include Area Code) (202) 767-4935 22c. OFFICE SYMBOL AFOSR/NA

DD FORM 1473, 83 APR EDITION OF 1 JAN 73 IS OBSOLETE

Unclassified

SECURITY CLASSIFICATION OF THIS PAGE

GRADUATE AERONAUTICAL LABORATORIES
of the
CALIFORNIA INSTITUTE of TECHNOLOGY
Pasadena, California 91125

ACTIVE FEEDBACK INTERACTION WITH A SHEAR LAYER

by

P. E. Dimotakis[1] and M. M. Koochesfahani[2]

AFOSR Grant No. AFOSR-84-0120

Annual Progress Report

30-June-86

---

1. Professor, Aeronautics & Applied Physics, California Institute of Technology (Principal Investigator).

2. Research Fellow, Aeronautics, California Institute of Technology

1. INTRODUCTION

Work over the past 12 months concentrated on further characterization of the effects of the actuator (pitching airfoil) on the shear layer structure and growth under open loop forcing. We also conducted a separate investigation into the structure of the wake of an oscillating airfoil in a steady, uniform free stream. This separate study was motivated by the wealth of interesting new phenomena we had observed in this flow, see our 1985 Annual Progress Report. Results are described below.

2. SHEAR LAYER FORCING

The flow visualization pictures presented in our 1985 Annual Progress Report showed that the interaction between the pitching airfoil and the shear layer could lead to large changes in the shear layer growth. We have studied this interaction further by looking at the effects of forcing on the regions both downstream and upstream of the airfoil over a wide range of airfoil oscillation frequencies, f. The flow geometry for the results described here is shown in figure 1. The velocity of the high-speed stream was set to $U_1 = 24$ cm/sec, corresponding to a low-speed stream velocity of $U_2 = 12$ cm/sec. The shear layer natural instability frequency at the splitter plate was estimated based on photographs to be approximately $f_0 = 7.5$ Hz under these conditions.

Figure 2 shows the effect of the pitching airfoil on the shear layer in the region downstream of the airfoil. In comparing with the natural layer, it can be seen that the presence of the non-oscillating airfoil in the shear layer has very little effect on the shear layer growth rate. When the forcing frequency is small ($f/f_0 << 1$), the layer growth rate is substantially increased as can be seen for the case $f = 0.25$ Hz. The region of the flow that shows increased growth rate moves upstream as the forcing frequency goes up. For example, in the

cases of f = 4 and 6 Hz (f/f_o = 0.53, 0.80 respectively) in figure 2, the part of the shear layer that is mostly affected has moved upstream of the airfoil as shown in figure 3. At these relatively high forcing frequencies, the layer growth rate, see figure 2, seems to be slightly lower than the natural case.

The portion of the shear layer upstream of the airfoil corresponding to the conditions in figure 2 is shown in figure 3. Note that the presence of the non-oscillating airfoil does not seem to alter the layer compared to the natural case. The same can be said about the cases with low-frequency forcing. At higher oscillation frequencies, for example f = 4 and 6 Hz in figure 3, control over the structure and growth rate in the upstream part of the layer can be exercised. In fact, many of the features documented in forced mixing layers (e.g. Ho & Huerre 1984) have also been observed here. We believe, however, that this is the first time the use of localized upstream forcing for mixing layer modification is reported. This is to be contrasted with previous methods of acoustical forcing (e.g. Zaman & Hussain 1982) or oscillating one or both free-stream velocities (Ho & Huang 1982 and Roberts & Roshko 1985).

The overall indication is that the frequency of the airfoil for which the largest effects are observed at a given station seems to correspond to the local vortex passage frequency of the natural layer at that station. In both cases of upstream and downstream forcing, the passing frequency of the large vortices that are finally formed is the same as the forcing frequency. In other words, if ℓ is the vortex spacing, $U_c = 0.5(U_1+U_2)$ the convection speed and f the forcing frequency, we obtain $f\ell/U_c = 1$. While there are some general similarities between these results and the previous work of Oster & Wygnanski (1982), we believe that the effects observed here are larger. Under low-frequency excitation, a layer growth rate increase of up to a factor of two over the natural case has been reported. In our data of figure 2, the growth rate in the case of f = 0.25 Hz is estimated to be

2.3 times that of the natural case. By increasing the forcing amplitude (airfoil pitch amplitude), higher values of growth rate of up to 2.6 times the natural growth rate seem to be possible, see figure 4. In this figure, it can be seen that the size of the structures has become comparable to the channel height. It is quite possible that the finite size of the channel may be restricting the growth of the structures to even larger sizes.

In order to get an estimate of the effect of the finite channel height on the shear layer growth rate, the linear inviscid stability analysis described in our research progress and forecast report 1984 was extended to include the finite channel boundary conditions. Using the linear inviscid stability approach for this purpose was motivated by the work of Oster & Wygnanski (1982) and Gaster et al. (1985) suggesting that the large structure behavior in the turbulent mixing layer may be described in part by an inviscid linear instability. A hyperbolic tangent velocity profile was used to calculate the wave-number, the amplification rate and the frequency of the most amplified disturbance as a function of channel height. In the results shown in figure 5, δ_ω is the layer vorticity thickness and 2H is the channel height. Since the visual thickness δ_{vis} of the shear layer is approximately $2\delta_\omega$, the horizontal axis in figure 5 is equivalent to the ratio of the layer visual thickness to the channel height $\delta_{vis}/2H$. All the instability quantities are normalized by the corresponding values when the walls are at infinity. From the curve of the amplification rate as a function of the channel height in figure 5, we estimate that as a result of the finite channel size the growth of the layer is reduced by about 20% in the case of figure 4, the bottom photograph, where the large vortex has filled roughly 70% of the channel height.

The results of this part of our effort have been submitted for presentation at the AIAA 25th Aerospace Sciences Meeting in Reno, Nevada, January 1987.

3. PITCHING AIRFOIL IN A UNIFORM FREE STREAM

We have continued the study of the vortical flow patterns in the wake of our pitching NACA 0012 airfoil, where we consider both sinusoidal and non-sinusoidal pitch waveforms. The main result has been that a great deal of control can be exercised on the structure of the wake of an airfoil in pitch oscillation. This is done by the control of the frequency, amplitude and also the shape of the oscillation waveform (see Koochesfahani 1985) which allows the modification of the wake structure through manipulation of the strength (circulation) and spacing of the vortices shed into the wake. At a given frequency, by simply changing the shape of the waveform, it is possible to generate a variety of complex vortex-vortex interactions. These interactions and the resulting wake structure can be very sensitive to small changes in the waveform shape. The strong dependence of the wake vortical patterns on the initial conditions, we suspect, may be related to the chaotic motions that occur when more than three vortices are present in the flow (see Aref 1983).

In what follows, we report new results for the case of sinusoidal pitch oscillations around the 1/4-chord point with the mean angle of attack set to zero. The airfoil chord is $C = 8$ cm and the free-stream velocity is $U_\infty = 15$ cm/sec resulting in a chord Reynolds number of 12,000 and a reduced frequency of $k = 2\pi fC/2U_\infty = 1.67$ (f/Hz). The oscillation frequency, f, and amplitude, A, are independently controlled through a closed-loop feedback servo system (see our 1985 Annual Report).

The sequence of pictures in figure 6 is a summary of the wake flow patterns when the oscillation amplitude is $A = 4$ degrees (i.e. the angle of attack varies between -4 and +4 degrees). Particular attention is drawn to the vortex patterns for frequencies larger than $f = 3.0$ Hz. In these cases, the vortex with a positive (counter-clockwise) circulation is located on top and the one with negative circulation on the bottom. This arrangement is opposite that of a typical Karman

vortex street observed in wakes and, in fact, this pattern corresponds to a two-dimensional "jet". In order to confirm this, a laser-Doppler (LDV) survey of the velocity field in the wake of the airfoil at a downstream station of X/C = 1 is shown in figure 7. It can be seen that the usual wake profile with a velocity deficit (i.e. case of airfoil with drag) can be transformed into a wake with excess momentum (no longer a wake but actually a jet, i.e. an airfoil with thrust) above a certain oscillation frequency. It is interesting to note that there exists a frequency (figure 7, f = 4.0 Hz) at which the wake has no deficit (momentumless wake, i.e. an airfoil with no drag). This condition corresponds to when the alternating vortices are positioned exactly on a straight line.

Another interesting feature has been the discovery of an axial flow along the cores of the wake vortices, see figure 8. The four dye streaks in this plan view of the wake are placed roughly symmetrically with respect to the water channel centerline and are approximately one chord length apart. The magnitude of the axial flow appears to depend on both the frequency and amplitude of oscillation and is believed to be tied directly to the vortex circulation. For example, figure 8 shows the increase of the axial velocity when the frequency is increased as manifested by the shortening of the distance downstream of the airfoil trailing edge where the axial flow in the vortices reaches the channel centerline. The dependence of this distance, denoted by L, on the oscillation frequency was derived from plan view photographs and is shown in figure 9. The nature of the vortex core axial flow is not very well understood. The origin of this phenomenon may lie in the interaction of a concentrated two-dimensional vortex with a bounding wall (in this case, the water channel side walls). The preliminary indications from our observations are that this may be a wave phenomenon at the start, and connected with the recent theoretical work of Lundgren & Ashurst (1985)

An estimate of the average axial celerity, W, along the vortex cores is presented in figure 10. The values of W were calculated from the L/C data of figure 9 assuming a constant axial speed and a vortex convection speed of U_c using the relation $W/U_c = 1.9/(L/C)$. In this expression, L is the distance downstream of the airfoil trailing edge where the axial flow in the vortices reaches the channel centerline. The constant 1.9 is a geometric factor resulting from the positions of the dye streaks in the plan view pictures (e.g. see figure 8). For the range of parameters studied here, the vortex convection speed U_c varies very little and is close to the free-stream speed U_∞ so that W/U_c in figure 10 is approximately equal to W/U_∞. The data in figure 10 indicate that the magnitude of the axial speed increases almost linearly with the oscillation frequency. Comparing results at the same frequency and two different oscillation amplitudes indicates a possible linear dependance on the amplitude also. It should be noted that the magnitude of the axial flow can be a sizable fraction of the free-stream velocity ($W/U_\infty \approx 0.65$).

Preliminary results of this part of our study were presented in the 38th annual meeting of the American Physical Society, Division of Fluid Dynamics (APS/DFD) in Tucson, Arizona, November 24-26, 1985 (see Koochesfahani 1985). A poster containing the flow visualization pictures of this study was selected as a winning entry in the Third Annual Picture Gallery Contest at this meeting. A more complete description of our results has been submitted for presentation at the AIAA 25th Aerospace Sciences Meeting in Reno, Nevada, January 1987.

4. WORK IN PROGRESS

We have recently added a real-time 2-D digital imaging capability to our data acquisition system. The motivation behind this development is two-fold. First, because the dynamics of the plane mixing layer are known to be dominated by large scale structures, input to the

closed-loop feedback control algorithm containing real-time global field information may be beneficial, if not essential. This information could take the form of an appropriate flow visualization image of the part of the shear layer being manipulated. Second, characterizing the many different vortical patterns observed for the case of non-sinusoidal pitch oscillation of the airfoil in uniform stream and their downstream evolution can be facilitated using real-time digital images in conjunction with image processing techniques.

At the present time, a Reticon 100×100 image array is used to acquire digital image data. The data acquisition system, shown in figure 11, uses a high-speed A/D system (in-house design) to digitize the output of the 2-D array to 8 bits in real-time and transfer the resulting digital data to memory or high-speed disk. A sample of the data obtained by this system is shown in figures 12 and 13. The data, in this case, were digitized and transferred into memory at a rate of 800 kByte/sec corresponding to an array framing rate of 80 frame/sec. Such high data rate capability has been realized by the recent modifications of our data acquisition system by Dr. D. Lang. The horizontal extent of the flow corresponds to 11.4 cm in figure 12 and 17.3 cm in figure 13 and the shear layer flow parameters are the same as those described earlier in section 2. The jaggedness of the pictures is mainly due to the simple one-level thresholding that was used so that the data could be output on a plotter. Note that in figure 13 only one out of every 8 frames of data is shown. Figures 12 and 13 show that most of the dynamically important features of the flow can be resolved in space and tracked in time under the current experimental conditions

In the investigations presently in progress, the LDV velocity data such as figure 7 are obtained using a computer-controlled data acquisition system. As shown schematically in figure 11, the Doppler burst is processed by a Tracking Phase-Locked Loop (TPLL, in-house design) whose output frequency is measured by a Real Time Clock card interfaced to the computer. We are now in the process of extending this

single-channel system to a 4-channel system (made of 4 TPLLs) to accommodate the multi-point velocity measurement capability needed for the feedback phase of this work.

5. REFERENCES

AREF, H. 1983 Integrable, chaotic and turbulent vortex motion in two-dimensional flows. Ann. Rev. Fluid Mech. 15, 345-389.

DIMOTAKIS, P. E. & KOOCHESFAHANI, M. M. 1985 Active feedback interaction with a shear layer. AFOSR-84-0120 Annual Progress Report.

GASTER, M., KIT, E. & WYGNANSKI, I. 1985 Large-scale structures in a forced turbulent mixing layer. J. Fluid Mech. 150, 23-39.

HO, C-M. & HUANG, L-S. 1982 Subharmonics and vortex merging in mixing layers. J. Fluid Mech. 119, 443-473.

HO, C-M. & HUERRE, P. 1984 Perturbed free shear layers. Ann. Rev. Fluid Mech. 16, 365-424.

KOOCHESFAHANI, M. M. 1985 The wake structure of an oscillating airfoil. Bull. Am. Phys. Soc. 30(10), 1717 (paper CE4).

LUNDGREN, T. S. & ASHURST, W. T. 1985 Area varying waves on curved vortex tubes. Bull. Am. Phys. Soc. 30(10), 1717 (paper CE6).

OSTER, D. & WYGNANSKI, I. 1982 The forced mixing layer between parallel streams. J. Fluid Mech. 123, 91-130.

ROBERTS, F. A. ROSHKO, A. 1985 Effects of periodic forcing on mixing in turbulent shear layers and wakes. AIAA-85-0570.

ZAMAN, K. B. M. Q. & HUSSAIN, A. K. M. F. 1981 Turbulence suppression in free shear flows by controlled excitation. J. Fluid Mech. 103, 133-159.

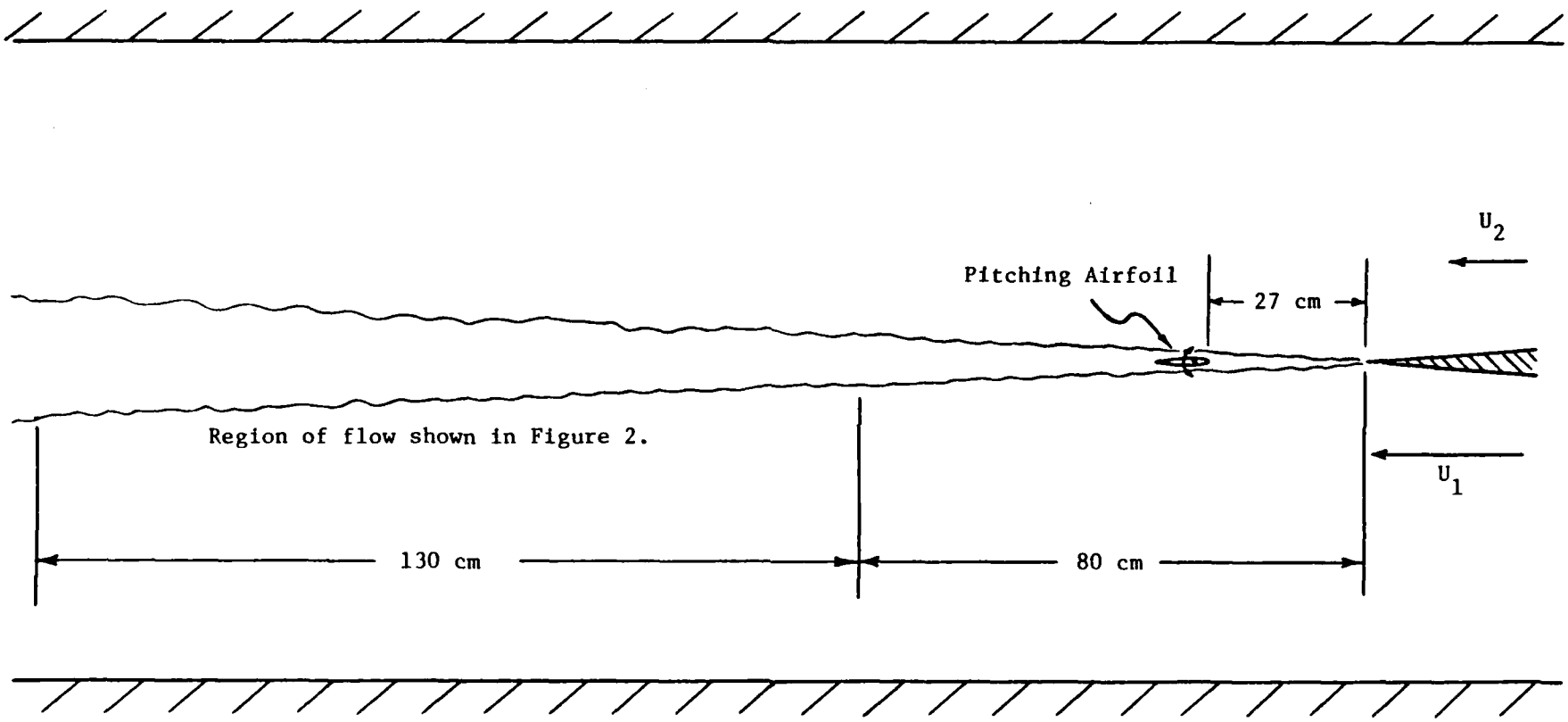

Figure 1. Flow Geometry for Shear Layer Forcing Experiments.

Natural shear layer (airfoil removed)

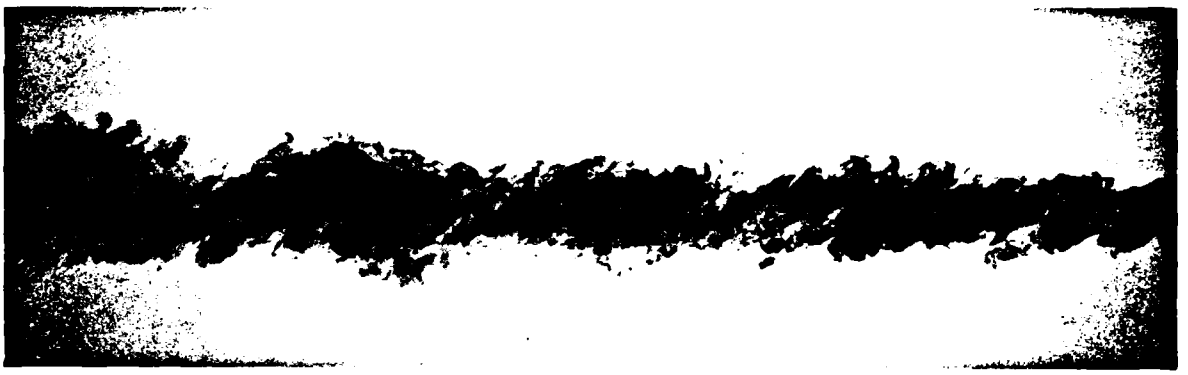

f = 0.0 Hz, A = 0 deg.

f = 0.25 Hz, A = 2 deg.

Figure 2. Effect of the Pitching Airfoil on the Shear Layer Structure and Growth in the Region Downstream of the Airfoil.

f = 0.50 Hz, A = 2 deg.

f = 4.0 Hz, A = 2 deg.

f = 6.0 Hz, A = 2 deg.

Figure 2. Continued.

Natural shear layer (airfoil removed)

f = 0.0 Hz, A = 0 deg.

f = 0.25 Hz, A = 2 deg.

f = 0.50 Hz, A = 2 deg.

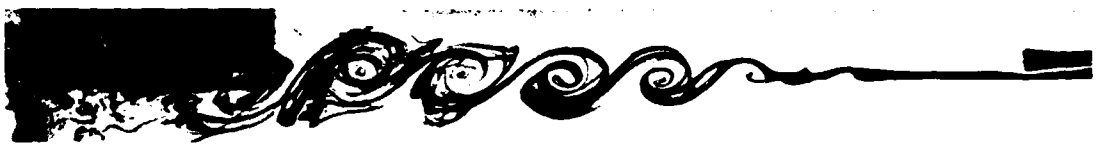

f = 4.0 Hz, A = 2 deg.

f = 6.0 Hz, A = 2 deg.

Figure 3. Effect of the Pitching Airfoil on the Shear Layer Structure and Growth in the Region Upstream of the Airfoil.

f = 0.25 Hz, A = 2 deg.

f = 0.25 Hz, A = 4 deg.

Figure 4. Effect of the Airfoil Pitch Amplitude on the Shear Layer Structure and Growth in the Region Downstream of the Airfoil.

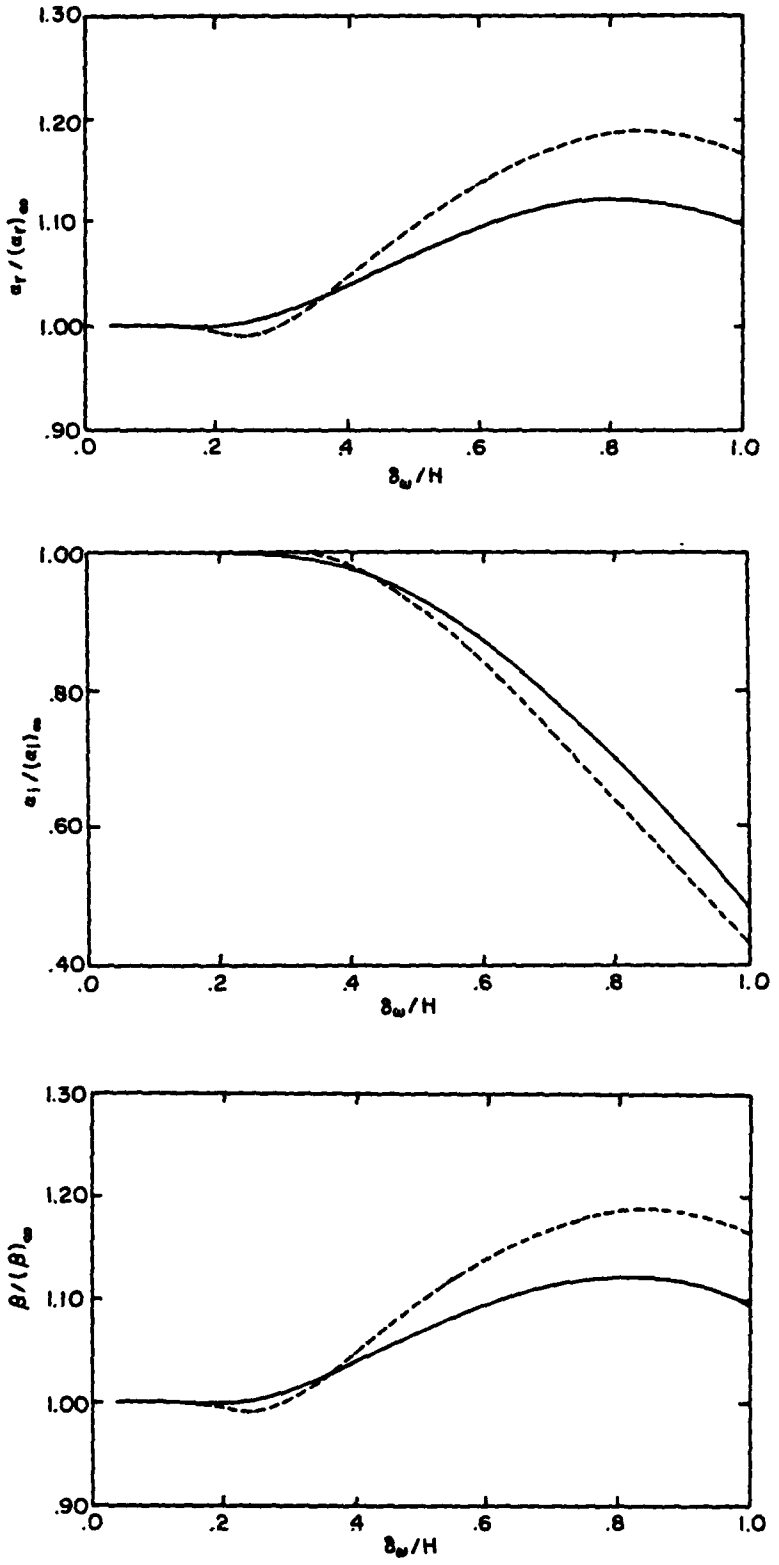

Figure 5. Effect of Finite Channel Height on the Wavenumber, Amplification Rate and Frequency of the Most Amplified Disturbance.
--- $U_2/U_1 = 0.0$ —— $U_2/U_1 = 0.5$

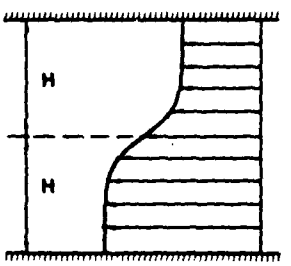

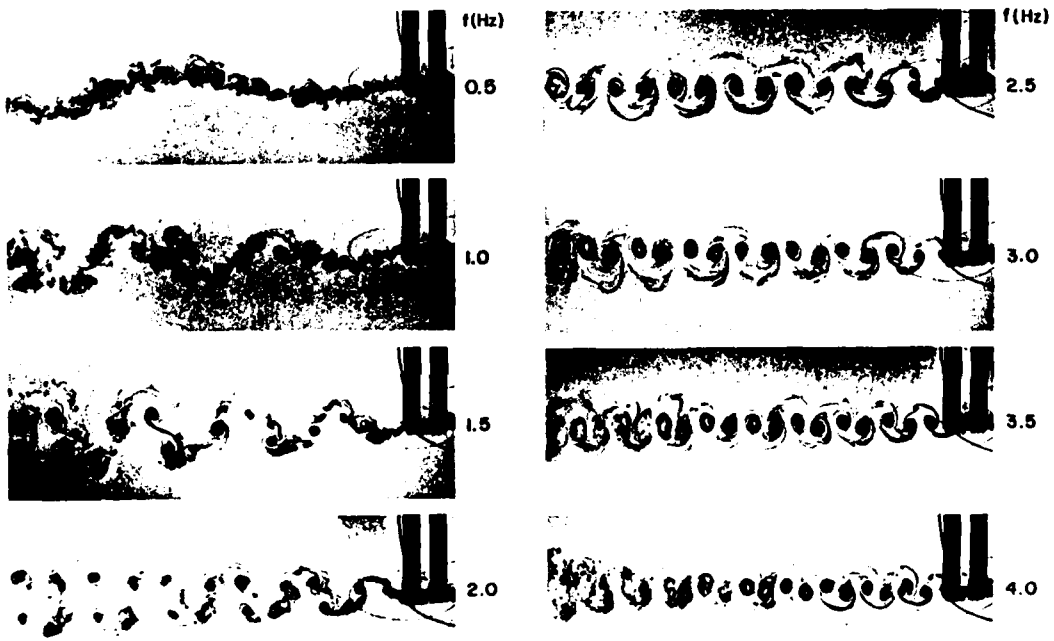

Figure 6. Wake of a NACA 0012 Airfoil Pitching Sinusoidally about 1/4 Chord Point. A = 4 degrees.

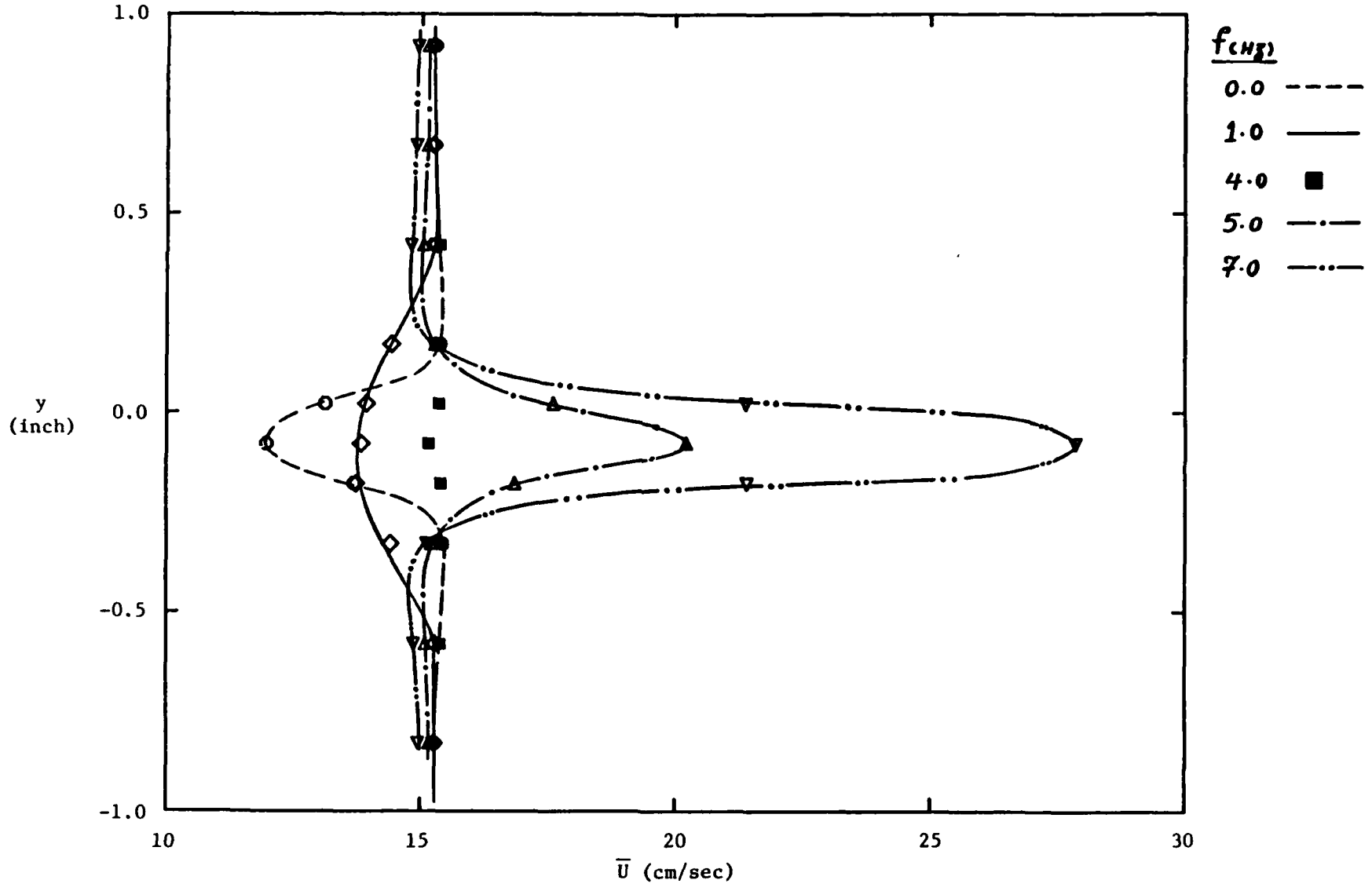

Figure 7. Mean Streamwise Velocity Profiles in the Wake of a Sinusoidally Pitching NACA 0012 Airfoil. Downstream Measurement Location is at 1 Chord Length Behind the Trailing Edge of the Airfoil.

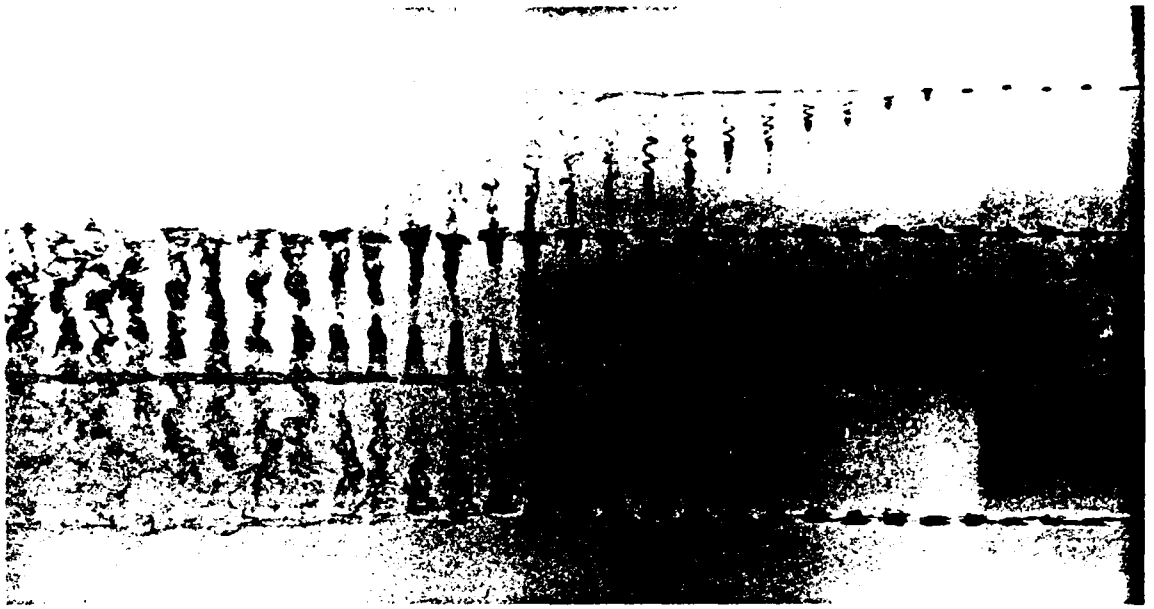

A = 2 degrees, f = 4.5 Hz

A = 2 degrees, f = 5.5 Hz

Figure 8. Axial Flow Along the Vortex Cores (Sinusoidal Oscillation).

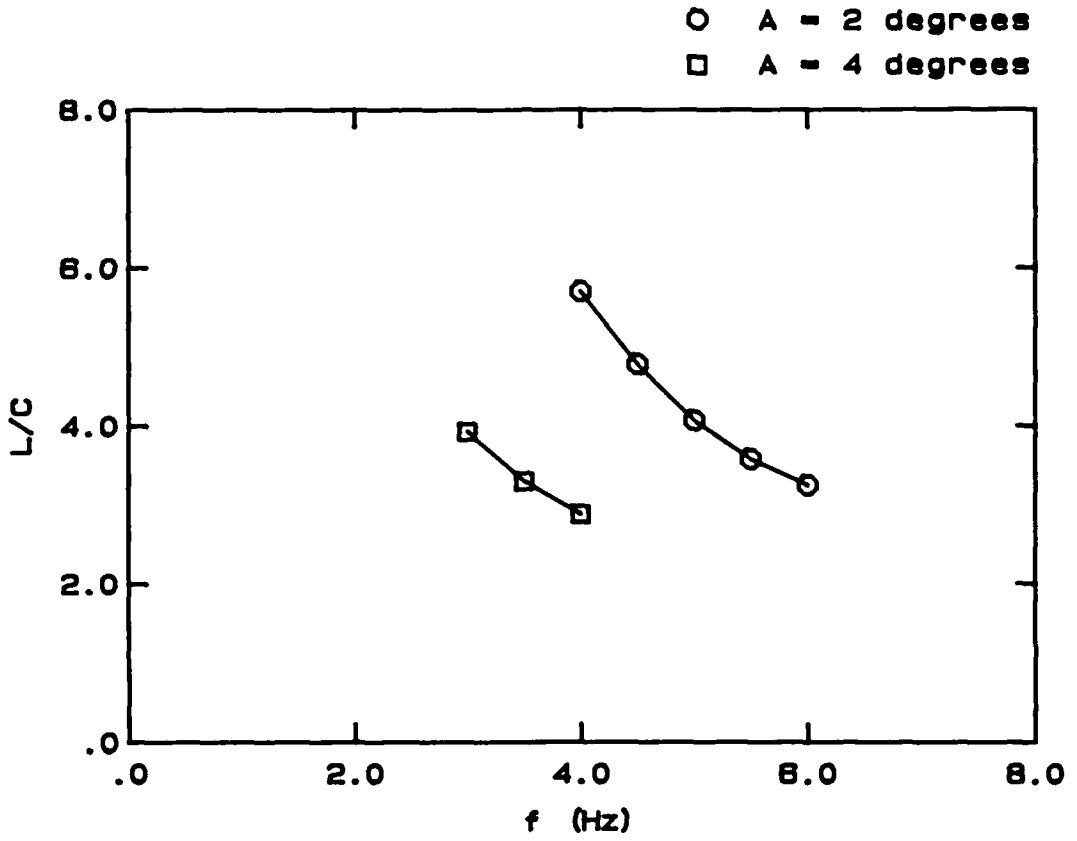

Figure 9. Estimate of the Downstream Distance Behind the Airfoil Where the Axial Flow in the Vortex Cores Reaches the Channel Midspan.

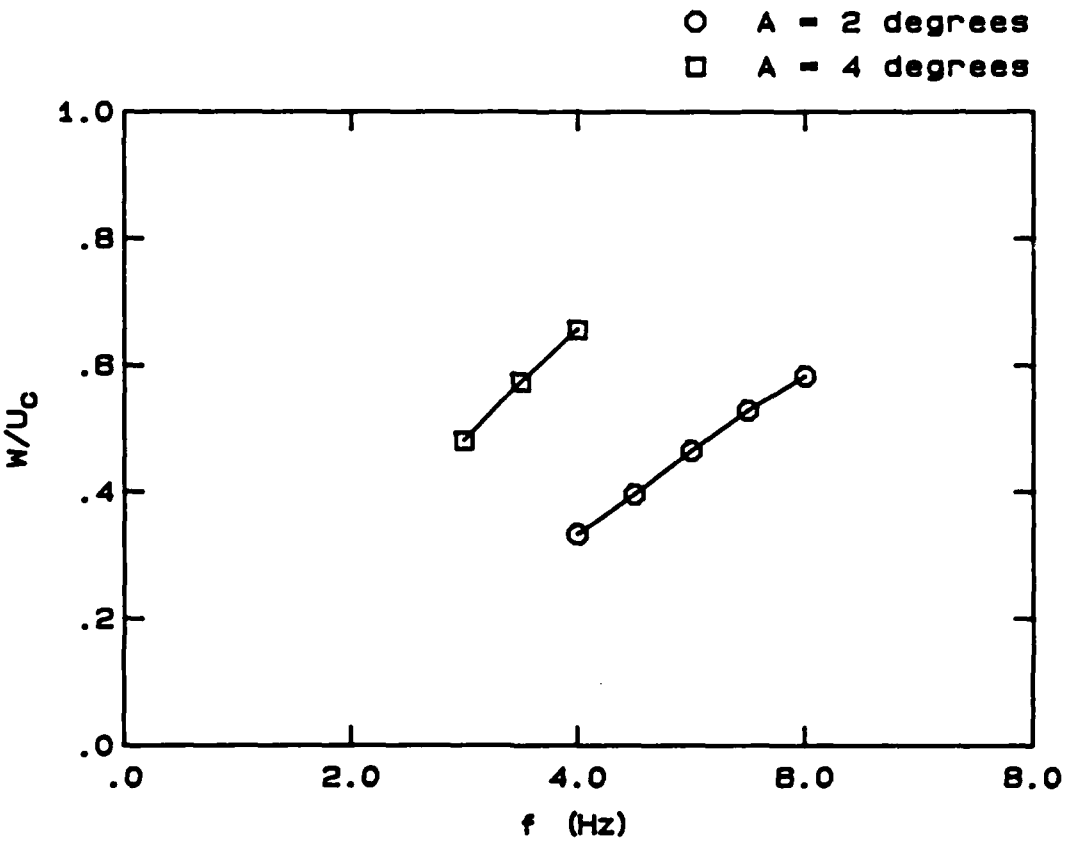

Figure 10. Estimate of the Magnitude of the Axial Celerity Along Vortex Cores.

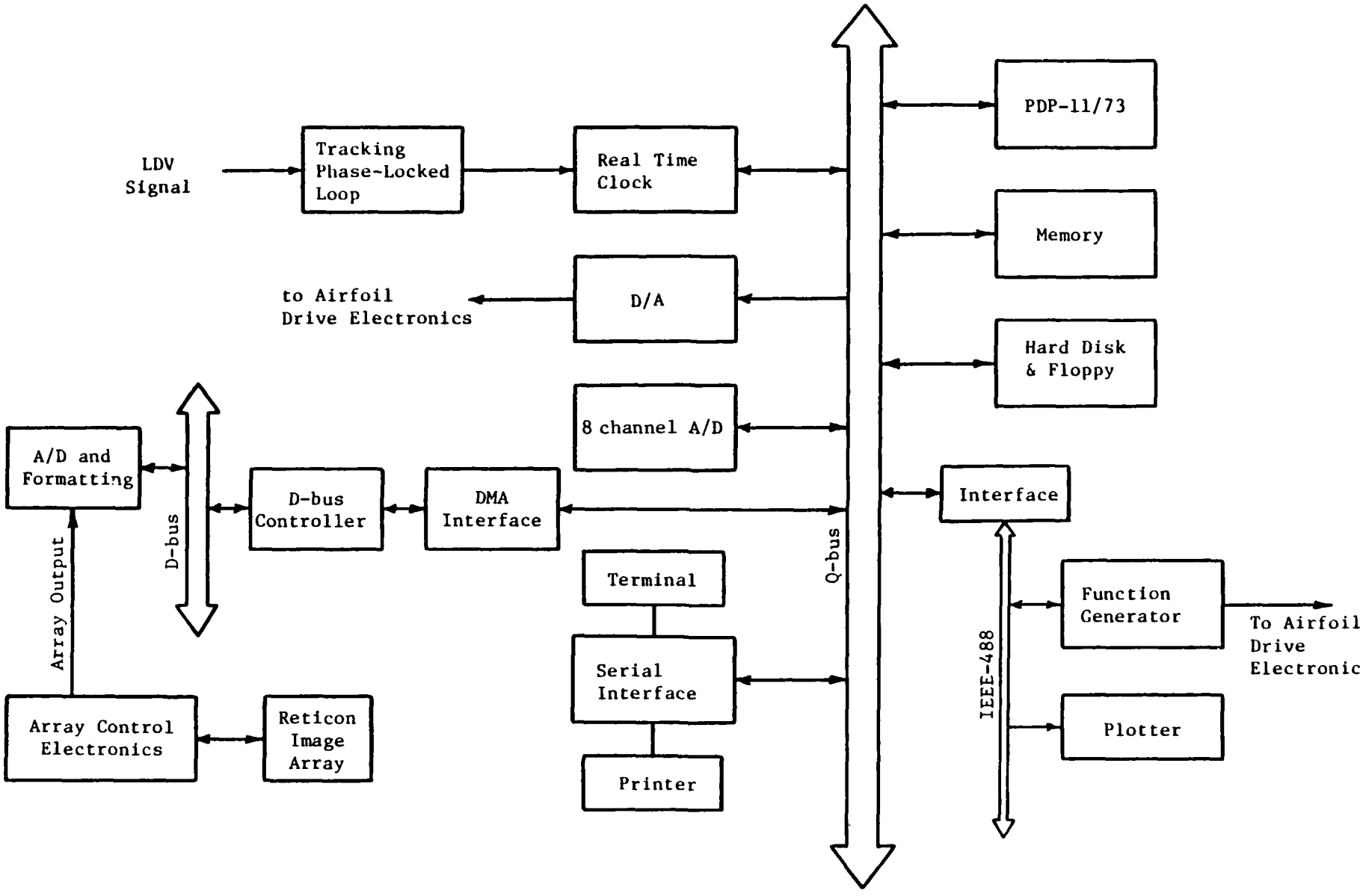

Figure 11. Schematic of Data Acquisition System.

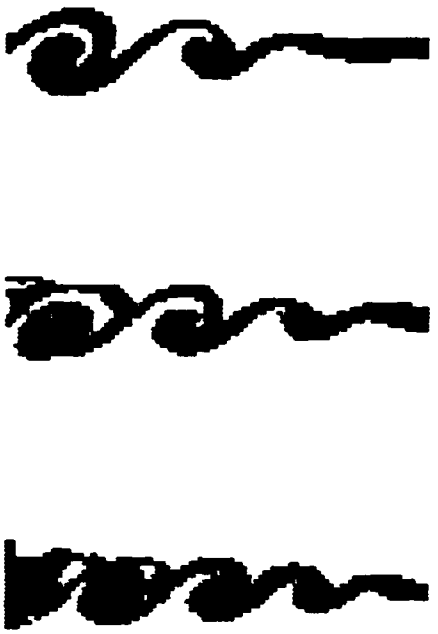

Figure 12. Digital Pictures of the Forced Mixing Layer.

Figure 13. Digital Pictures of the Time Evolution of the Forced Mixing Layer. Forcing Frequency f = 4 Hz; Pictures are 0.1 second apart with Time Increasing from Top to Bottom.

END

12-86

DTIC